



# Histological validation of simultaneous non-contrast angiography and intraplaque hemorrhage imaging (SNAP) for characterizing carotid intraplaque hemorrhage

Dongye Li<sup>1</sup> · Huiyu Qiao<sup>2</sup> · Yongjun Han<sup>2,3</sup> · Hualu Han<sup>2</sup> · Dandan Yang<sup>2,3</sup> · Jingli Cao<sup>4</sup> · Huimin Xu<sup>5</sup> · Tao Wang<sup>6</sup> · Yajie Wang<sup>7</sup> · Jun Shen<sup>1</sup> · Xihai Zhao<sup>2</sup>

Received: 27 May 2020 / Revised: 17 August 2020 / Accepted: 24 September 2020 / Published online: 14 October 2020  
© European Society of Radiology 2020

## Abstract

**Objectives** This study sought to validate the performance of simultaneous non-contrast angiography and intraplaque hemorrhage (SNAP) imaging in characterizing carotid IPH by histology.

**Methods** Thirty-five patients with carotid atherosclerotic disease (symptomatic 50–70% stenosis or > 70% stenosis) scheduled for carotid endarterectomy underwent 3.0-T carotid MR imaging by acquiring SNAP and magnetization-prepared rapid acquisition gradient-echo (MP-RAGE) sequences. Presence and area of IPH were separately evaluated on SNAP and MP-RAGE images. Presence and area of IPH were also assessed on histology. Agreement between SNAP/MP-RAGE and histology was determined in identify and quantify IPH using Cohen kappa, Spearman correlation, and Bland-Altman analyses.

**Results** Of all 35 patients (mean age: 63.1 ± 8.8 years; 27 males), 128 slices with successful registration were eligible for analysis. The accuracy, sensitivity, specificity, and positive and negative predictive values were 86.7%, 85%, 89.6%, 93.2%, and 78.2% for SNAP, and 76.6%, 75%, 79.2%, 85.7%, and 65.5% for MP-RAGE in identification of IPH, respectively. In identification of IPH, the kappa value between SNAP and histology and between MP-RAGE and histology was 0.725 and 0.520, respectively. The correlation between SNAP and histology ( $r = 0.805, p < 0.001$ ) was stronger than that between MP-RAGE and histology ( $r = 0.637, p < 0.001$ ) in measuring IPH area. Bland-Altman analysis showed that, in measuring IPH area, the bias of SNAP (1.4 mm<sup>2</sup>, 95% CI: - 0.016 to 2.883) was smaller than that of MP-RAGE (1.7 mm<sup>2</sup>, 95% CI: - 0.039 to 3.430) compared with histology.

**Conclusions** This validation study by histology demonstrates that SNAP sequence better identifies and quantifies carotid intraplaque hemorrhage compared with traditional MP-RAGE sequence.

## Key Points

- SNAP imaging showed better agreement with histology compared with MP-RAGE imaging, especially for the IPHs with small size.
- SNAP sequence is a more effective tool to identify and quantify carotid IPH than traditional sequence of MP-RAGE that can help clinicians to optimizing the treatment strategy.

---

Jun Shen and Xihai Zhao contributed equally to this work.

---

✉ Jun Shen  
shenjun@mail.sysu.edu.cn

✉ Xihai Zhao  
xihai Zhao@tsinghua.edu.cn

<sup>1</sup> Department of Radiology, Sun Yat-Sen Memorial Hospital, Sun Yat-Sen University, No. 107 Yanjiang Road West, Guangzhou 510120, China

<sup>2</sup> Center for Biomedical Imaging Research, Department of Biomedical Engineering, Tsinghua University School of Medicine, Haidian District, Beijing 100084, China

<sup>3</sup> Beijing Institute of Brain Disorders, Laboratory of Brain Disorders, Ministry of Science and Technology, Collaborative Innovation Center for Brain Disorders, Capital Medical University, Beijing, China

<sup>4</sup> China National Clinical Research Center for Neurological Diseases, Beijing Tiantan Hospital, Capital Medical University, Beijing, China

<sup>5</sup> Department of Radiology, Peking University Third Hospital, Beijing, China

<sup>6</sup> Department of Neurosurgery, Peking University Third Hospital, Beijing, China

<sup>7</sup> Department of Clinical Laboratory, Beijing Ditan Hospital, Capital Medical University, Beijing, China

- *The plaque components of rich lipid pools or loose matrix and chronic/old IPH (cholesterol crystals) can lead to false positive and false negative results in SNAP and MP-RAGE imaging for identifying IPH.*

**Keywords** Carotid artery · Atherosclerotic plaque · Magnetic resonance imaging

### Abbreviations

CEA	Carotid endarterectomy
IPH	Intraplaque hemorrhage
MP-RAGE	Magnetization-prepared rapid acquisition gradient-echo
PSIR	Phase-sensitive inversion-recovery reconstruction
SNAP	Simultaneous non-contrast angiography and intraplaque hemorrhage

### Introduction

It has been shown that intraplaque hemorrhage (IPH) is one of the key features of carotid vulnerable atherosclerotic plaques [1–3]. Many previous prospective studies in various populations demonstrated that presence of IPH accelerates plaque progression and increases the risk of ischemic cerebrovascular events [4–8]. In addition, investigators found that, for patients with carotid IPH, stenting therapy group developed more fresh ipsilateral silent ischemic lesions than carotid endarterectomy (CEA) group, suggesting that CEA might be a better treatment for carotid plaques with IPH [9]. Recent studies also reported that the size and magnetic resonance (MR) signal intensity of carotid IPH were strongly correlated with clinical events [10, 11]. Therefore, qualitative and quantitative assessment of IPH may help to provide more precise information for stratifying the risk of cerebrovascular events and optimizing patient management.

Traditionally, the assessment of carotid IPH is mainly based on the T1-weighted MR imaging techniques, such as time of flight (TOF), T1-weighted (T1W), and MP-RAGE imaging sequences. Among these T1-weighted sequences, MP-RAGE has been demonstrated to have the highest sensitivity and accuracy in detecting carotid IPH validated by histology [12]. Recently, a novel imaging sequence of simultaneous non-contrast angiography and intraplaque hemorrhage (SNAP) has been proposed for simultaneously providing non-contrast MR angiography and identification of IPH in carotid arteries [13]. Most recently, Li et al have demonstrated that SNAP imaging can detect more IPHs compared with MP-RAGE, particularly for small IPHs [14]. However, the comprehensive usefulness of SNAP imaging in identification and quantification of carotid IPH has not been validated by histology. This study sought to histologically validate the performance of SNAP imaging in assessing carotid IPH compared with MP-RAGE imaging.

### Materials and methods

#### Study population

Patients with carotid atherosclerotic stenosis who were scheduled to carotid endarterectomy (CEA) at Peking University Third Hospital were recruited in this study. The included patients had either cerebrovascular symptoms (stenosis  $\geq 50\%$ ) or asymptomatic severe stenosis (stenosis  $\geq 70\%$ ) in carotid arteries. The exclusion criteria were as follows: (1) claustrophobia; (2) contraindications to MR imaging; and (3) critical conditions such as coma, heart failure, or respiratory failure. All included patients underwent carotid MR imaging at Center for Biomedical Imaging Research of Tsinghua University within 1 week before CEA. The clinical characteristics such as age, gender, history of smoking, hypertension, diabetes, and stroke were collected from medical record. The levels of high-density lipoprotein (HDL), low-density lipoprotein (LDL), total cholesterol (TC), and triglyceride (TG) were also recorded. The study protocol was approved by institutional review board and written consent form was obtained from all subjects.

#### Carotid MR imaging protocol

Carotid MR imaging was performed on a whole-body 3.0 T MR scanner (Achieva TX, Philips Healthcare) with a dedicated 8-channel carotid coil. The images of carotid arteries were acquired using a multicontrast vessel wall imaging protocol with the following parameters: (1) three-dimensional TOF: fast field echo (FFE), TR/TE 20/5.5 ms, flip angle  $20^\circ$ ; (2) quadruple-inversion-recovery T1W imaging: turbo spin echo (TSE), TR/TE 800/10 ms, flip angle  $90^\circ$ ; (3) multislice double inversion-recovery T2-weighted imaging (T2W MDIR): TSE, TR/TE 4800/50 ms, flip angle  $90^\circ$ ; (4) MP-RAGE: FFE, TR/TE 13.2/3.2 ms, flip angle  $15^\circ$ ; (5) SNAP: FFE, TR/TE 9.98/6.11 ms, flip angle  $11^\circ$ . The TOF, T1W, T2W, MP-RAGE, and SNAP images were acquired cross-sectionally centered at the bifurcation of index carotid arteries with an identical field of view (FOV)  $160 \times 160 \text{ mm}^2$ . The slice thickness was 2 mm for T1W, T2W, and TOF imaging and 1 mm for SNAP and MR-RAGE imaging, respectively. The longitudinal coverage was 32 mm for T1W and T2W imaging and 48 mm for TOF, MP-RAGE, and SNAP imaging, respectively. The imaging parameters are detailed in Table 1. The index artery was defined as carotid artery with moderate to severe stenosis which was referred to CEA treatment.

**Table 1** Carotid artery MR imaging parameters

	T1W	T2W	3D TOF	MP-RAGE	SNAP
Acquisition	TSE	TSE	FFE	TFE	FFE
TR/TE (ms)	800/10	4800/50	20/5.5	13.2/3.2	9.98/6.11
Black-blood	QIR	MDIR	–	–	PSIR
Flip angle (deg)	90	90	20	15	11
Orientation	Axial	Axial	Axial	Axial	Axial
FOV (mm)	160 × 160 × 32	160 × 160 × 32	160 × 160 × 48	160 × 160 × 48	160 × 160 × 48
Resolution (mm)	0.6 × 0.6 × 2	0.6 × 0.6 × 2	0.6 × 0.6 × 2	0.6 × 0.6 × 1	0.8 isotropic
NSA	1	1	1	2	1
Scan time (min)	6	4	2	4	2

*FFE* fast field echo, *TSE* turbo spin echo, *QIR* quadruple-inversion recovery, *MDIR* multislice double inversion recovery, *PSIR* phase-sensitive inversion recovery, *TR* repeat time, *TE* echo time, *FOV* field of view, *NSA* number of signal averaged

### Specimen processing and histological image review

The specimens of carotid plaques were obtained from a routine CEA procedure and fixed in 10% neutral buffered formalin within 4 h after excision, decalcified in 10% formic acid, and embedded a bloc in paraffin. After CEA, the specimens were sectioned (10 µm) every 0.5 mm throughout the length of the specimen and stained (hematoxylin and eosin [H&E]). The histological images were interpreted by two histologists with > 5 years' experience in pathologic analysis of carotid plaque who were blinded to MR image review (C.J. and W.Y.). The presence of IPH was determined and the area of the IPH was measured using ImageJ software and published criteria [15].

### Image matching between MRI and histology

The histological images were matched to the MR images by the histologist (C.J.) who evaluated the histological images and an MR reviewer (Q.H.) with 3 years' experience in carotid artery imaging who was not involved in image review of this study. Given the difference in slice thickness between the MR image slices (2 mm) and the histological sections (10 µm, every 0.5 mm), four histological sections were matched with one cross-sectional MR image on the basis of the relative distance from the bifurcation. Considering the potential shrinkage of the CEA specimen during histological processing, additional modification was used for matching MR image with histology. The Landmarks such as the relative distance from carotid bifurcation and morphological features of lumen, vessel wall, and calcifications were used for co-registration [16].

### Image analysis

All carotid MR images, which were matched to the histologic specimens, were interpreted by two radiologists with

consensus who had more than 3 years' experience in vascular imaging blinded to clinical information and histological specimens. The presence and the size of IPHs of carotid artery on MP-RAGE and SNAP images were evaluated by using ImageJ software [17]. The IPH on MP-RAGE or SNAP images was defined as hyperintense compared with adjacent muscle (signal intensity ratio  $\geq 1.5:1$ ) [18]. The image review was conducted with two steps: step 1, reviewers (L.D. and Y.D.) outlined IPH on SNAP images blinded to MR-RAGE images and other contrast-weighted images; and step 2, reviewers (L.D. and Y.D.) outlined IPH on MP-RAGE images blinded to SNAP images and other contrast-weighted images 1 month later. The purpose of having 1-month time interval between these two rounds of image review was to minimize the memory bias. The area of IPH on MP-RAGE and SNAP images for each axial location was also measured. The image quality (IQ) of MR images was rated using 4-point scale (from poor to excellent) and those images with poor IQ (IQ = 1) will be excluded [19].

After reviewed all carotid MR imaging, we marked positive-false and negative-false finding in identification of IPH by SNAP and MP-RAGE imaging compared with histology. In the process of histology image interpretation, histologists were blinded to the MR imaging. For MR images with positive-false finding, we analyzed the histological components corresponding to area showing hyperintense signal on the MR images. Similarly, on the MR images with negative-false finding, we analyzed the type of IPH and the surrounding components on histology. We routinely interpreted the following plaque components on histology: lipid pool, loose matrix, calcification, obsolete bleeding, etc.

### Statistical analysis

Continuous variables were presented as mean and standard deviation and discrete variables were described as frequency.

The number and area of IPHs measured by SNAP and MP-RAGE images and histology were calculated and compared. A shrinkage artifact of 7.8% induced by histological preparation was determined to minimize the bias in quantitative measurements [20]. The agreement between SNAP and histology and between MP-RAGE and histology in identifying presence or absence of IPH was determined using Cohen's kappa analysis. The kappa values between MR imaging and histology with different thresholds of IPH area were also calculated. Different thresholds were chosen in determining the agreement between MR imaging and histology to test if the MR imaging had different performance in IPH detection. The thresholds of IPH area were calculated before the analysis as the area ( $A$ ) of a circle where the radius was an increment of the image spatial resolution (0.60 mm, Table 1):  $A = \pi \cdot (0.60x)^2$ , where  $x$  was 1.5, 2.0, 2.5, or 3.0 (yielding cutoff values of 2.54, 4.52, 7.07, or 10.17 mm<sup>2</sup>, respectively) [12]. The agreement and associations of IPH area measured by MP-RAGE and SNAP images with histology were determined using Spearman rank correlation coefficients and Bland-Altman analyses.

The kappa values were corresponding to the following agreement levels: 0.01–0.20, slight agreement; 0.21–0.40, fair agreement; 0.41–0.60, moderate agreement; 0.61–0.80, good agreement; and 0.81–1.00, excellent agreement. A  $p$  value < 0.05 was considered as statistically significant. All statistical analyses were performed using SPSS 22.0 (IBM SPSS Statistics software).

## Results

A total of 35 patients (mean age:  $63.1 \pm 8.8$  years; age range: 37–81 years; 27 males) from May 2017 to October 2017 were recruited in this study. Of 35 patients, 77.1% (27/35) are male, 42.9% (15/35) had hypertension, 17.1% (6/35) had history of smoke, 5.7% (2/35) had diabetes, and 68.6% (24/35) had stroke. The clinical characteristics of this study population are detailed in Table 2.

### Agreement of SNAP and MP-RAGE in identification of IPH with histology

Of the 35 patients, 630 histological sections were obtained and stained. Of the 630 sections, 128 were successfully matched with carotid MR images with acceptable image quality for statistical analysis. Of the 128 matched sections, 80 (62.5%) were found to have IPH on histology. Of the 128 matched slices, 73 (57.0%) were found to have IPH on SNAP imaging. Of these 73 corresponding slices, 68 (93.2%) were classified as IPH positive on histology. Of the 128 matched slices, 70 (54.7%) were found to have IPH on MP-RAGE imaging. Of these 70 corresponding slices, 60 (85.7%) were classified as

IPH positive on histology. Of the 55 IPH negative slices on SNAP imaging, 43 (78.2%) were classified as IPH negative and 12 (22.8%) were classified as IPH positive on histology, respectively. Of the 58 IPH negative slices on MP-RAGE imaging, 38 (65.5%) were classified as IPH negative and 20 (34.5%) were classified as IPH positive on histology, respectively (Table 3). In detecting IPH, the kappa value between SNAP and histology and between MP-RAGE and histology was 0.725 (95% CI, 0.603–0.846, Table 3) and 0.520 (95% CI, 0.372–0.668, Table 3), respectively. The accuracy, sensitivity, specificity, positive predictive value, and negative predictive value were 86.7%, 85%, 89.6%, 93.2%, and 78.2% for SNAP imaging, and 76.6%, 75%, 79.2%, 85.7%, and 65.5% for MP-RAGE imaging in identification of IPH, respectively.

The kappa values at different thresholds of IPH areas (2.54, 4.52, 7.07, and 10.17 mm<sup>2</sup>) between SNAP and histology and between MP-RAGE and histology are presented in Fig. 1. The agreement increased with the increase of threshold of IPH areas between SNAP imaging and histology and between MP-RAGE imaging and histology. Of note, SNAP imaging showed higher kappa values compared with MP-RAGE imaging in detection of IPH at any threshold of IPH area. For example, when detecting IPH with area  $\geq 10.17$  mm<sup>2</sup>, the kappa value was 0.860 between SNAP imaging and histology and 0.660 between MP-RAGE imaging and histology, respectively (Fig. 1).

In identification of IPH by SNAP and MP-RAGE imaging, 80.0% (4/5) and 58.3% (7/12) false positive findings were due to the presence of lipid pools and loose matrix confirmed by histology, respectively. In identification of IPH by SNAP and MP-RAGE imaging, the false negative findings were due to the presence of calcification and chronic/old IPH (cholesterol crystals) confirmed by histology. The influence factors of false positive/negative findings in identification of IPH by SNAP and MP-RAGE imaging are detailed in Table 4.

### Agreement of SNAP and MP-RAGE in quantification of IPH with histology

Of 80 MR images matched with histological sections with IPH, 57 (71.3%) were found to have IPH on both SNAP and MP-RAGE images. On these 57 images, the area of IPH measured by SNAP and MP-RAGE imaging and histologic specimen was  $16.8 \pm 13.8$  mm<sup>2</sup> and  $17.2 \pm 11.3$  mm<sup>2</sup> and  $12.6 \pm 7.5$  mm<sup>2</sup> respectively (Fig. 2). Bland-Altman analysis revealed that, in measuring the area of IPH, the bias of SNAP (mean value, 1.4 mm<sup>2</sup>, 95% CI: – 0.016 to 2.883) was smaller than that of MP-RAGE (mean value, 1.7 mm<sup>2</sup>, 95% CI: – 0.039 to 3.430) compared with histology (Fig. 3). Bland-Altman plots show that the bias in measuring the IPH area between MRI and histology increased with size of IPH (Fig. 3). Spearman rank correlation analysis revealed that the correlation between SNAP and histologic specimens ( $r = 0.805$ ,  $p < 0.001$ ) was

**Table 2** Clinical characteristics of the study population (*n* = 35)

	Mean ± SD or <i>n</i> (%)	Range if applicable
Gender, male	27 (35)	
Age, years	63.1 ± 8.8	29–82
Hypertension	15 (42.9)	
Systolic pressure, mmHg	137.7 ± 20.8	97–196
Diastolic pressure, mmHg	74 ± 10.0	53–92
Hyperlipidemia	10 (28.6)	
High-density lipoprotein, mmol/L	1.0 ± 0.2	0.7–1.3
Low-density lipoprotein, mmol/L	2.4 ± 0.9	1.3–4.3
Total triglyceride, mmol/L	1.8 ± 0.9	0.8–2.7
Total cholesterol, mmol/L	4.0 ± 1.4	2.7–6.2
Diabetes	2 (5.7)	
History of cardiovascular disease	4 (11.4)	
History of stroke	24 (68.6)	
History of smoke	6 (17.1)	

stronger than that between MP-RAGE and histologic specimens ( $r = 0.637, p < 0.001$ ) in measuring the IPH area. Figure 4 represents examples showing IPH on MP-RAGE and SNAP images and histologic section.

### Discussion

In this study, we investigated and compared the performance of SNAP and MP-RAGE imaging in evaluating carotid IPH validated by histology. In identification of carotid IPH, SNAP imaging showed better agreement with histology compared with MP-RAGE imaging, especially for the IPHs with small size. In quantifying the area of IPH, SNAP imaging also showed better agreement and smaller bias than MP-RAGE imaging in comparing with histology. Our results suggest that SNAP imaging might be a more sensitive and accurate

imaging approach in assessing carotid IPH than MP-RAGE imaging.

In the present study, SNAP imaging showed higher sensitivity in identifying presence of IPH compared with MP-RAGE sequence. A comparison study by Ota et al reported that MP-RAGE imaging had higher sensitivity (53%) and specificity (97%) compared with TOF (sensitivity: 35%; specificity: 96%) and T1W imaging (sensitivity: 47%; specificity: 92%) in identification of IPH [12]. In the present study, the capability of MP-RAGE in detecting IPHs (sensitivity: 75%; specificity: 79%) was comparable with literature reports when balancing sensitivity and sensitivity, whereas SNAP imaging had improved sensitivity (85%) and specificity (90%) in detecting IPHs compared with MP-RAGE. SNAP is primarily designed for IPH imaging by using optimized parameters with phase-sensitive inversion-recovery reconstruction (PSIR). In previous study, Wang et al demonstrated that the SNAP

**Table 3** Agreement between MR imaging and histology in identifying IPH

		Histology		Total
		Absence	Presence	
SNAP	Absence	43	12	55
	Presence	5	68	73
MP-RAGE	Absence	38	20	58
	Presence	10	60	70
Total		48	80	128

SNAP: accuracy, sensitivity, and specificity are 86.7%, 85%, and 90%, respectively.  $k = 0.725$  (95% CI, 0.603–0.846). MP-RAGE: accuracy, sensitivity, and specificity are 76.6%, 75%, and 79%, respectively.  $k = 0.520$  (95% CI, 0.372–0.668)

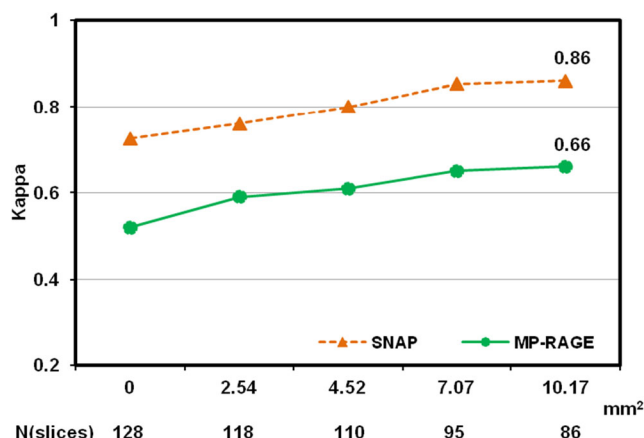


**Fig. 1** The kappa values for agreement between SNAP and histology and between MR-RAGE imaging and histology at different threshold of IPH areas



**Table 4** The influence factor of false positive/negative findings in identification of IPH by SNAP and MP-RAGE imaging

False positive	Lipid pools/loose matrix	Calcification	Poor stability of blood suppression	Unexplainable
SNAP ( <i>n</i> = 5)	4	1	0	0
MP-RAGE ( <i>n</i> = 12)	7	3	0	2
False negative	Chronic/old IPH	Calcification	Poor stability of blood suppression	Unexplainable
SNAP ( <i>n</i> = 17)	5	6	4	2
MP-RAGE ( <i>n</i> = 24)	8	8	8	0

sequence significantly improved intraplaque hemorrhage-wall contrast-to-noise ratio ( $p < 0.01$ ) and blood suppression efficiency ( $p < 0.01$ ) using optimized PSIR technique and TI parameters [13]. In addition, the signal of other plaque components, such as calcification and lipid, and the adjacent sternocleidomastoid muscle signal were set to an intermediate signal ( $Mz = 0$ ) in SNAP sequence with PSIR technique [21]. Therefore, with increased IPH-wall contrast, investigators found that SNAP can detect smaller IPH which may not be detected by MP-RAGE [14].

To our knowledge, the size of IPH might be one of the most important factors that influence the performance of MR imaging techniques in detecting IPH. When the size of IPH is smaller, the impact of partial volume due to insufficient MR spatial resolution and the overlap of surrounding tissue (calcification) signals tend to be obvious. On the contrary, when the size of IPH is larger, the proportion of paramagnetic hemosiderin is higher, which will lead to stronger hyperintense signal and achieve better detection performance. In the present study, we found the kappa values for both SNAP and MP-RAGE sequences in detecting IPH were consistently improved as IPH size increased validated by histology. When excluded MR slices with  $< 2.54 \text{ mm}^2$ ,  $4.52 \text{ mm}^2$ ,  $7.07 \text{ mm}^2$ , and  $10.17 \text{ mm}^2$ , the kappa values between SNAP and histology and between MP-RAGE and histology increased and finally reached 0.86 and 0.66 after excluded MR slices with  $< 10.17 \text{ mm}^2$ , respectively. Our findings are in line with the

reports from a study by Ota et al in which three T1-weighted MR sequences (TOF, FSE and MP-RAGE) were compared in detecting carotid IPH with different size validated by histology [12]. In addition, the kappa value ( $k = 0.80$ ) between MP-RAGE imaging and histology in the study by Ota et al is higher than that of our present study. This difference may be due to the fact that the MR imaging slices with heavily calcified IPHs in the study by Ota et al were excluded. Clearly, calcification within plaques will strongly disturb identification of IPH in MP-RAGE imaging.

In the present study, both SNAP and MP-RAGE imaging sequences had false positive and negative findings in some cases. We have analyzed the cases with false positive findings in identification of IPH by SNAP and MP-RAGE and found that the main components of such plaques were lipid pools and loose matrix. Previous studies have shown that loose matrix may shorten the T1 value to some extent, and show hyperintense signal which is similar to the IPH [22, 23]. Since both SNAP and MP-RAGE are heavily T1-weighted sequence, it is expected the plaque components of loose matrix was mimicked as IPH in some cases. However, few studies have confirmed the signal appearance of the lipid pool of carotid plaque on the MR imaging. The present study suggests that lipid pool may shorten the T1 value which is similar to loose matrix, which became one of the reasons for false positive results of SNAP and MP-RAGE imaging in IPH detection (Fig. 5). A large number of histological comparative studies are needed to confirm in the future. We also analyzed the cases having false negative findings in identification of IPH by SNAP and MP-RAGE imaging. We found that the presence of calcification and chronic/old IPH (cholesterol crystals) were the major components on histology. Chronic/old hemorrhage usually prolongs T1 value and shows isointense or hypointense on T1 sequence [24] which cannot be detected by MP-RAGE and SNAP imaging (Fig. 6a). Previous studies have shown that calcification can also interfere with the identification of IPH by T1 sequences such as MP-RAGE imaging. Since the application of PSIR technology to SNAP imaging can ignore the influence of small calcifications in identifying IPH, the accuracy of SNAP imaging tends to be higher than that of MP-RAGE imaging in identification of IPH (Fig. 6b). In addition, poor stability of blood suppression is another reason for the false positive finding of IPH by MP-

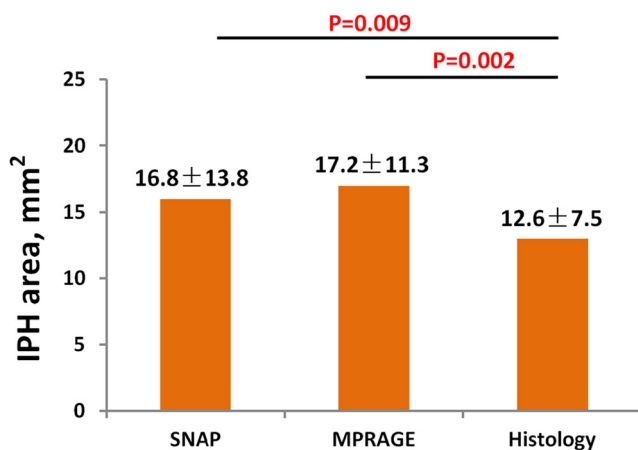


**Fig. 2** Comparison of IPH area between SNAP and MP-RAGE and histology

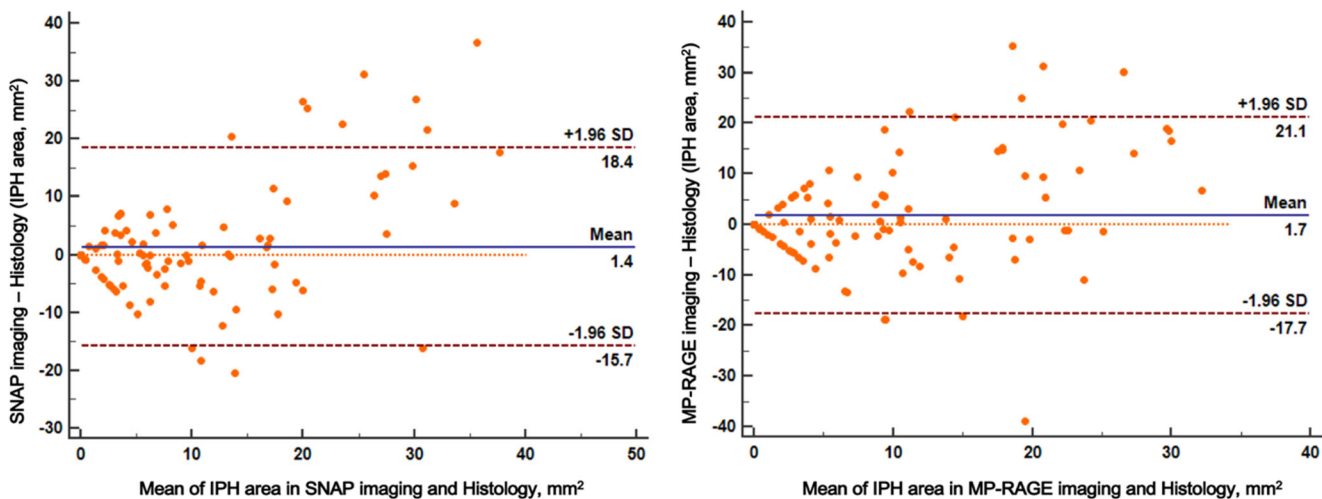


Fig. 3 Bland-Altman plots for testing the bias of SNAP and MP-RAGE images in measuring IPH area with the reference of histology

RAGE sequence. In contrast, the stability of blood suppression of SNAP imaging is better than MP-RAGE. Hence, SNAP imaging had better performance in identification of IPH with lower false positive and negative values compared with MP-RAGE imaging.

Few studies have reported on the agreement of measuring IPH size between SNAP imaging and histology. Using an optimal threshold, Liu et al found the volume of IPH measured by SNAP and that measured by histology were correlated (Spearman’s rho = 0.76,  $p = 0.002$ ) [25]. In the present

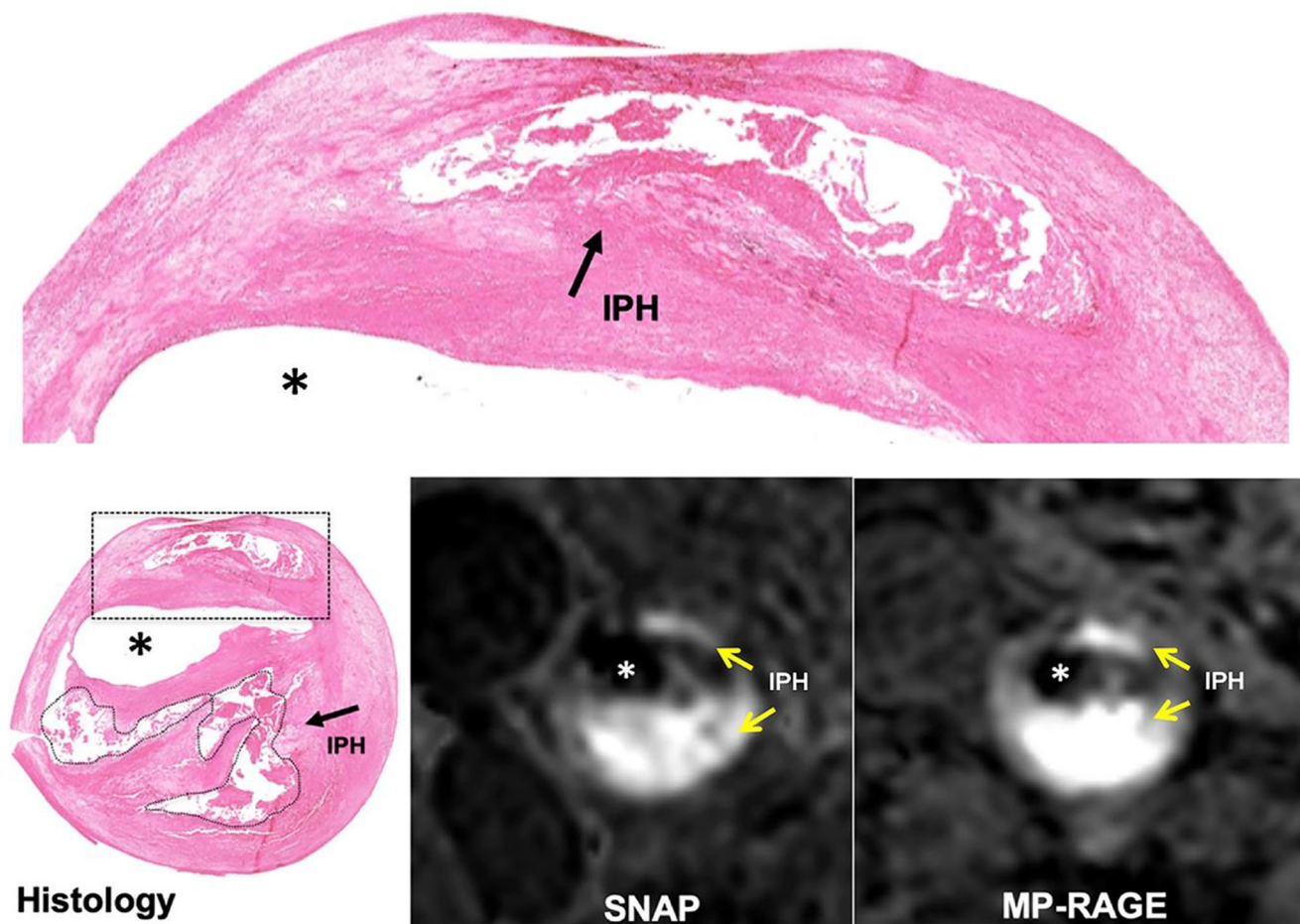
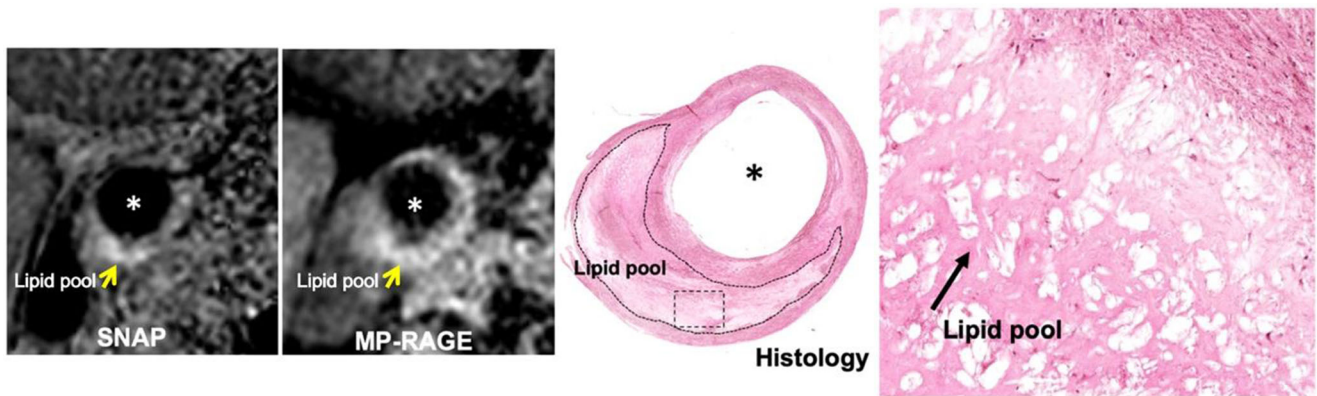


Fig. 4 Represents examples showing IPH (arrow) on MP-RAGE and SNAP images and histology. \* = lumen





**Fig. 5** The components of rich lipid pool (arrow), which were mimicked as IPH, show hyperintense on both MP-RAGE and SNAP imaging. \* = lumen

study, we also separately measured the size of IPH on SNAP images, MP-RAGE images, and histologic specimens for slices with IPH. We found that SNAP imaging showed stronger correlation with histology than MP-RAGE imaging in measuring IPH size ( $r = 0.805$  vs.  $r = 0.637$ ,  $p < 0.001$ ). It can be seen from the Bland-Altman analysis that, compared with histology, SNAP imaging had smaller bias in measuring the area of IPH compared with MP-RAGE imaging (mean value of bias,  $1.4 \text{ mm}^2$  vs.  $1.7 \text{ mm}^2$ ). The IPH was quantified manually when hyperintense signal present on MP-RAGE or SNAP images. The contour of IPH delineated on SNAP

images might be more accurate than that on MP-RAGE images because MP-RAGE might underestimate IPH size due to the insufficient IPH-wall CNR [21]. In this study, we also found that the IPH areas measured by SNAP and MP-RAGE imaging were larger than that of histology. In the process of histologic specimen of carotid plaque, the volume of sample and each component within the plaque will shrink to a certain extent. In the process of dehydration and staining of sample, some unstable IPHs may fall off which will further lead to shrinkage. We found that the bias in measuring the IPH area between MRI and histology increased with size on

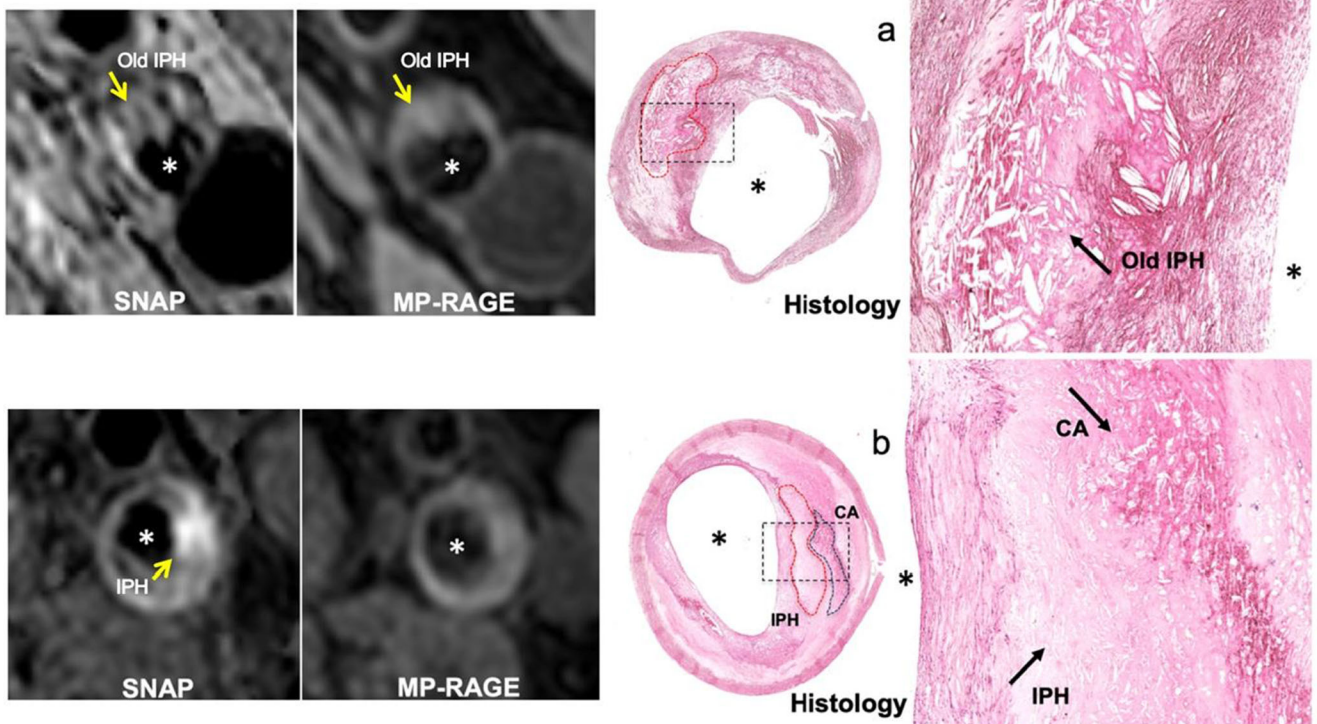


**Fig. 6** Old hemorrhage (a, arrow) shows isointense or hypointense which cannot be detected by MP-RAGE and SNAP imaging. The histologic section from a patient shows that calcification exists around IPH (b,

arrow), and it was not detected by MP-RAGE imaging but well delineated by SNAP imaging (hyperintense). \* = lumen



Bland-Altman plots. In general, the larger the size of IPH, the greater the complexity due to conjunct with other plaque components, such as calcification. If the larger size IPH was affected by the surrounding calcification, the local signal intensity will be dropped [12], and the SNAP and MP-RAGE imaging will subsequently underestimate the area of IPH. If the larger size IPH was conjunct with loose matrix and lipid pool, it may lead to an increase in the area of hyperintense signal and overestimation of the area of IPH [23]. Therefore, it can be explained why the IPH size bias measured by SNAP and MP-RAGE imaging increased with size of IPH. In addition, measuring area of IPH may be influenced by partial volume effects and susceptibility effect in SNAP and MP-RAGE imaging, which might play key roles in overestimation of the size of IPH. A previous study showed that the area of IPH on SNAP imaging was nearly 2 times larger than that of MP-RAGE [14]. However, in the present study, the mean IPH areas measured by SNAP and MP-RAGE imaging were similar ( $16.8 \pm 13.8 \text{ mm}^2$  and  $17.2 \pm 11.3 \text{ mm}^2$ ). We found that most of the IPHs in the present study were at the subacute and chronic stage on histology, suggesting that SNAP imaging and MP-RAGE imaging may have a good consistency in measuring the area of IPH in subacute and chronic stage. Future studies investigating the capability of SNAP imaging in identification of IPHs at different stage needs to be explored.

This study has several limitations. First, the number of carotid plaques with IPH was limited. Future studies with larger sample size of histological specimens are warranted. Second, the acquired resolution of SNAP imaging (isotropic 0.8 mm) may attenuate the accuracy of assessment of IPH, especially for small IPHs which can be improved by optimizing the spatial resolution from the technical aspect in future studies. Third, in this study, we defined IPH when there was hyperintense signal on MP-RAGE and SNAP imaging. However, some other factors may also influence the identification of IPH on MR imaging, such as blood suppression, calcification, and IPH stage. Comprehensive analysis in assessing IPH considering all above factors is suggested in future studies.

## Conclusions

This validation study by histology demonstrates that SNAP sequence better identifies and quantifies carotid intraplaque hemorrhage compared with traditional sequence of MP-RAGE.

**Funding** This study is supported by grants of Ministry of Science and Technology of China (2017YFC1307904), National Natural Science Foundation of China (81771825, U1801681), and Beijing Municipal Science and Technology Commission (D171100003017003), the Key Areas Research and Development Program of Guangdong (2019B020235001), Guangdong Province Universities, and Colleges Pearl River Scholar Funded Scheme (2017).

## Compliance with ethical standards

**Guarantor** The scientific guarantor of this publication is Xihai Zhao.

**Conflict of interest** The authors of this manuscript declare no relationships with any companies whose products or services may be related to the subject matter of the article.

**Statistics and biometry** No complex statistical methods were necessary for this paper.

**Informed consent** Written informed consent was obtained from all subjects (patients) in this study.

**Ethical approval** Institutional Review Board approval was obtained.

## Methodology

- retrospective
- observational
- multicenter study

## References

1. Michel JB, Virmani R, Arbustini E, Pasterkamp G (2011) Intraplaque haemorrhages as the trigger of plaque vulnerability. *Eur Heart J* 32:1977–1985
2. Takaya N, Yuan C, Chu B et al (2005) Presence of intraplaque hemorrhage stimulates progression of carotid atherosclerotic plaques: a high-resolution magnetic resonance imaging study. *Circulation* 111:2768–2775
3. Saam T, Cai J, Ma L et al (2006) Comparison of symptomatic and asymptomatic atherosclerotic carotid plaque features with in vivo MR imaging. *Radiology* 240:464–472
4. Altaf N, MacSweeney ST, Gladman J, Auer DP (2007) Carotid intraplaque hemorrhage predicts recurrent symptoms in patients with high-grade carotid stenosis. *Stroke* 38:1633–1635
5. Saam T, Hetterich H, Hoffmann V et al (2013) Meta-analysis and systematic review of the predictive value of carotid plaque hemorrhage on cerebrovascular events by magnetic resonance imaging. *J Am Coll Cardiol* 62:1081–1091
6. Gupta A, Baradaran H, Schweitzer AD et al (2013) Carotid plaque MRI and stroke risk: a systematic review and meta-analysis. *Stroke* 44:3071–3077
7. Sun J, Underhill HR, Hippe DS, Xue Y, Yuan C, Hatsukami TS (2012) Sustained acceleration in carotid atherosclerotic plaque progression with intraplaque hemorrhage: a long-term time course study. *JACC Cardiovasc Imaging* 5:798–804
8. Kampschulte A, Ferguson MS, Kerwin WS et al (2004) Differentiation of intraplaque versus juxtaluminal hemorrhage/thrombus in advanced human carotid atherosclerotic lesions by in vivo magnetic resonance imaging. *Circulation* 110:3239–3244
9. Hosseini AA, Kandiyil N, Macsweeney ST, Altaf N, Auer DP (2013) Carotid plaque hemorrhage on magnetic resonance imaging strongly predicts recurrent ischemia and stroke. *Ann Neurol* 73:774–784
10. Yamada K, Yoshimura S, Kawasaki M et al (2011) Embolic complications after carotid artery stenting or carotid endarterectomy are associated with tissue characteristics of carotid plaques evaluated by magnetic resonance imaging. *Atherosclerosis* 215:399–404
11. Wang X, Sun J, Zhao X et al (2017) Ipsilateral plaques display higher T1 signals than contralateral plaques in recently

- symptomatic patients with bilateral carotid intraplaque hemorrhage. *Atherosclerosis* 257:78–85
12. Ota H, Yamykh VL, Ferguson MS et al (2010) Carotid intraplaque hemorrhage imaging at 3.0-T MR imaging: comparison of the diagnostic performance of three T1-weighted sequences. *Radiology* 254:551–563
  13. Wang J, Bornert P, Zhao H et al (2013) Simultaneous noncontrast angiography and intraplaque hemorrhage (SNAP) imaging for carotid atherosclerotic disease evaluation. *Magn Reson Med* 69:337–345
  14. Li D, Zhao H, Chen X et al (2018) Identification of intraplaque haemorrhage in carotid artery by simultaneous non-contrast angiography and intraplaque haemorrhage (SNAP) imaging: a magnetic resonance vessel wall imaging study. *Eur Radiol* 28:1681–1686
  15. Lusby RJ, Ferrell LD, Ehrenfeld WK, Stoney RJ, Wylie EJ (1982) Carotid plaque hemorrhage. its role in production of cerebral ischemia. *Arch Surg* 117:1479–1488
  16. Yuan C, Mitsumori LM, Ferguson MS et al (2001) In vivo accuracy of multispectral magnetic resonance imaging for identifying lipid-rich necrotic cores and intraplaque hemorrhage in advanced human carotid plaques. *Circulation* 104:2051–2056
  17. Schneider CA, Rasband WS, Eliceiri KW (2012) NIH Image to ImageJ: 25 years of image analysis. *Nat Methods* 9:671–675
  18. Liu J, Balu N, Hippe DS et al (2016) Semi-automatic carotid intraplaque hemorrhage detection and quantification on magnetization-prepared rapid acquisition gradient-echo (MP-RAGE) with optimized threshold selection. *J Cardiovasc Magn Reson* 18:41
  19. Underhill HR, Yuan C, Terry JG et al (2008) Differences in carotid arterial morphology and composition between individuals with and without obstructive coronary artery disease: a cardiovascular magnetic resonance study. *J Cardiovasc Magn Reson* 10:1–11
  20. Virmani R, Kolodgie FD, Burke AP, Farb A, Schwartz SM (2000) Lesions from sudden coronary death: a comprehensive morphological classification scheme for atherosclerotic lesions. *Arterioscler Thromb Vasc Biol* 20:1262–1275
  21. Wang J, Ferguson MS, Balu N et al (2010) Improved carotid intraplaque hemorrhage imaging using a slab-selective phase-sensitive inversion-recovery (SPI) sequence. *Magn Reson Med* 64:1332–1340
  22. Dai Y, Lv P, Lin J et al (2017) Comparison study between multicontrast atherosclerosis characterization (MATCH) and conventional multicontrast MRI of carotid plaque with histology validation. *J Magn Reson Imaging* 45:764–770
  23. Fan Z, Yu W, Xie Y et al (2014) Multi-contrast atherosclerosis characterization (MATCH) of carotid plaque with a single 5-min scan: technical development and clinical feasibility. *J Cardiovasc Magn Reson* 16:53
  24. Chu B, Kampschulte A, Ferguson MS et al (2004) Hemorrhage in the atherosclerotic carotid plaque: a high-resolution MRI study. *Stroke* 35:1079–1084
  25. Liu J, Sun J, Balu N et al (2019) Semiautomatic carotid intraplaque hemorrhage volume measurement using 3D carotid MRI. *J Magn Reson Imaging* 50:1055–1062

**Publisher's note** Springer Nature remains neutral with regard to jurisdictional claims in published maps and institutional affiliations.